Article published online: 2021-07-30

Imaging in spinal posterior epidural space lesions: A pictorial essay

Foram B Gala[1,2], Yashant Aswani[3]

[1]Lifescan Imaging Centre, [3]Department of Radiology, TNMC and BYL Nair Charitable Hospital, Mumbai, Maharashtra, India, [2]Department of Neuroradiology, University Hospital of Zurich/Children's Hospital of Zurich, Zurich, Switzerland

Correspondence: Dr. Foram B Gala, Lifescan Imaging Centre, Malad, Mumbai - 400 064, Maharashtra, India.
E-mail: drforamgala@gmail.com

Abstract

Spinal epidural space is a real anatomic space located outside the dura mater and within the spinal canal extending from foramen magnum to sacrum. Important contents of this space are epidural fat, spinal nerves, epidural veins and arteries. Due to close proximity of posterior epidural space to spinal cord and spinal nerves, the lesions present with symptoms of radiculopathy and/or myelopathy. In this pictorial essay, detailed anatomy of the posterior epidural space, pathologies affecting it along with imaging pearls to accurately diagnose them are discussed. Various pathologies affecting the posterior epidural space either arising from the space itself or occurring secondary to vertebral/intervertebral disc pathologies. Primary spinal bone tumors affecting the posterior epidural space have been excluded. The etiological spectrum affecting the posterior epidural space ranges from degenerative, infective, neoplastic - benign or malignant to miscellaneous pathologies. MRI is the modality of choice in evaluation of these lesions with CT scan mainly helpful in detecting calcification. Due to its excellent soft tissue contrast, Magnetic Resonance Imaging is extremely useful in assessing the pathologies of posterior epidural space, to know their entire extent, characterize them and along with clinical history and laboratory data, arrive at a specific diagnosis and guide the referring clinician. It is important to diagnose these lesions early so as to prevent permanent neurological complication.

Key words: Compressive myelopathy; epidural space; magnetic resonance imaging; posterior epidural abscess; posterior epidural hematoma

Introduction

Spinal epidural space is a closed anatomic space between the dura mater and the bony spinal canal. It extends from the foramen magnum to the sacrum. Unlike its intracranial counterpart, spinal epidural space is real. The presence of anchoring plicae and meningovertebral ligaments divide the space into anterior, lateral and posterior compartments.[1] Owing to close proximity to cord and nerve roots, the lesions of epidural space present with symptoms of myelopathy and/or radiculopathy. Magnetic Resonance Imaging (MRI) is the imaging modality of choice to assess the spine and pathologies of posterior spinal epidural space. The clinical details, laboratory parameters and imaging characteristics help arrive at a specific diagnosis. In this pictorial review, we focus on the MRI features of lesions affecting the posterior spinal epidural space.

Anatomy

Spinal epidural space extends rostrally from the fusion of spinal and periosteal layers of dura mater at foramen magnum[2] up to the sacrococcygeal membrane caudally. The fusion of the former prevents intracranial extension.

Access this article online	
Quick Response Code:	Website: www.ijri.org
	DOI: 10.4103/0971-3026.190406

Cite this article as: Gala FB, Aswani Y. Imaging in spinal posterior epidural space lesions: A pictorial essay. Indian J Radiol Imaging 2016;26:299-315.

The space is limited ventrally by the posterior longitudinal ligament, posterior margins of vertebral bodies and intervertebral discs. The posterior margin is formed by ligamentum flavum, capsule of facet joints and laminae. Pedicles and intervertebral foraminae form the lateral boundaries [Figures 1 and 2].

Spinal epidural space is a real space at the intervertebral level, however, it is a potential space at the vertebral level where the dura fuses with the posterior longitudinal ligament and the annular ligament.[3] It is widest at upper thoracic levels where the posterior space measures 7.5 mm. The dimensions at C7–T1 and lumbar level are approximately 0.4 mm and 4–7 mm, respectively.[4] Both the size and shape of the space are dictated by the size and shape of the vertebral canal and position of the dural sac within. The space communicates freely with the paravertebral space via intervertebral foraminae.

Contents

Epidural fat

Epidural fat is the dominant component of posterior spinal epidural space and varies in direct proportion with rest of the body. The distribution of fat is uneven but predictable. It is abundant in dural sleeves along the nerve roots, sparse at C7–T1, T11–T12, and L2–L3 levels, and distinctly absent from within the dural sac. The epidural fat protects the cord within the dural sac and spinal nerves by buffering the pulsatile movements of the dural sac, facilitates dural sac movement over periosteum during flexion and extension, and creates reservoir for lipophilic substances.[5] The dural sac ends approximately at S2 level and contains the spinal cord and cauda equina. The fat is responsible for epidural space being wider posteriorly than anteriorly.

Nerves

Spinal nerves exit laterally through the intervertebral foramina on both sides. There are 8 cervical nerves and 7 cervical vertebrae, and nerves are numbered according to the vertebra below, except C8 nerve exits between C7 and D1 level. However, in thoracic, lumbar, and sacral regions, the nerves are numbered according to the vertebra above. Dorsal root ganglion is located laterally and enhances after gadolinium injection.

Vascular supply

The venous drainage is via Batson's plexus, which is located in the anterior epidural space. It comprises external and internal venous plexuses and intraosseous veins of vertebral column.[6,7] Both internal and external plexuses are composed of four interconnecting longitudinal veins; two anterior and two posterior. These veins have communications with intracranial, cervical, intercostal,

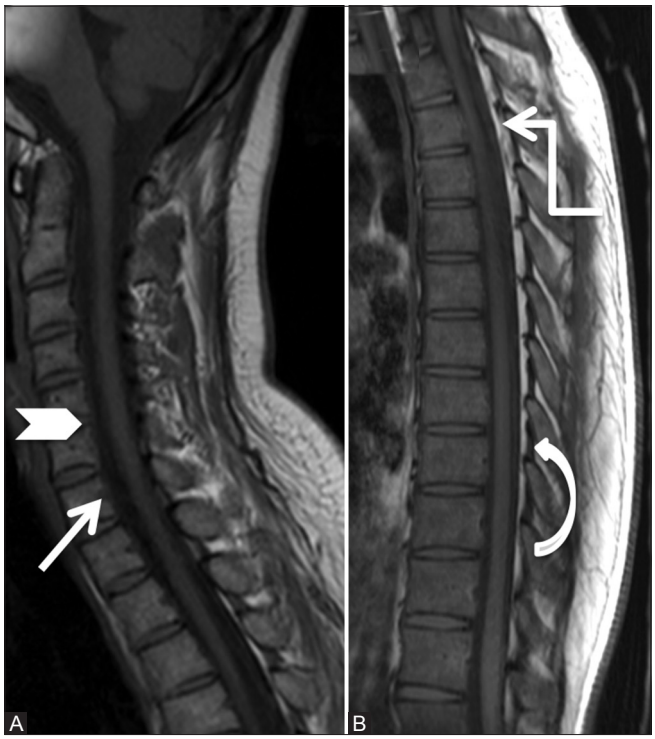

Figure 1 (A and B): Anatomy of epidural space: Sagittal T1-weighted images of cervical (A) and thoracic spine (B) showing posterior longitudinal ligament, posterior margin of vertebral bodies (arrow), and intervertebral discs (arrowhead) forming anterior margin of epidural space. The posterior margin is formed by ligamentum flavum (curved arrow), capsule of facet joints, and laminae. Note sheet-like posterior epidural fat in the dorsal spine (elbow arrow)

Figure 2 (A and B): Anatomy of epidural space: Sagittal (A) and axial T1-weighted (B) images of lumbar spine showing anterior boundary of the epidural space formed by posterior longitudinal ligament, posterior margin of vertebral bodies (arrow), and intervertebral discs (white arrowhead). Note the triangular shape of posterior epidural space in lumbar spine (elbow arrow). Pedicles and intervertebral foraminae (black arrowhead) form the lateral boundaries

lumbar and iliac veins. The drainage to the right atrium is via azygous vein.[8] Because the entire system is valveless and the lymphatics are sparse and concentrated along the dural roots, the route of spread of infection or malignancy to the epidural space is hematogenous. The posterior venous plexus is variable in size in the lumbar region and increases in the dorsal and cervical region.

There is anterior and posterior spinal arterial arcade formed from spinal arteries entering at each intervertebral foramen. These arise from vertebral arteries, thoracic and lumbar aorta; and anastomose with anterior spinal artery arising from vertebral artery.

The arteries in lumbar epidural space are branches of iliolumbar arteries. These are placed laterally in the space and hence escape trauma during epidural puncture.

Pathologies Affecting Posterior Spinal Epidural Space

The lesions may involve primarily the posterior epidural space or can be secondary to vertebral/intervebral disc pathology. Discussion of primary bone tumors affecting the posterior epidural space is beyond the scope of this article. Table 1 summarizes the various pathologies affecting the posterior spinal epidural space.

Degenerative [Figures 3-7]

Herniated disc

A degenerated disc may herniate into the anterior epidural space by virtue of perforation of the annulus fibrosis and posterior longitudinal ligament and loose contact with its parent disc (sequestration).[9] Once in the anterior epidural space, the disc fragment may migrate cranially, caudally, or laterally. Movement further posteriorly is restricted by meningovertebral ligaments. Migration to the posterior epidural space is a rare event. MRI with contrast is needed to diagnose this accurately. The disc fragment is hypointense on T1-weighted (T1W) images and hyperintense on T2W images compared to the parent disc. Reparative process, inflammation, and granulation tissue surround the disc fragment accounting for its peripheral enhancement. A tract-like enhancement extending from the outer aspect of the degenerated intervertebral disc to the posterior epidural space, indicating the route of migration virtually clinches the diagnosis[9] [Figures 3 and 4].

Table 1: Classification of pathologies affecting posterior spinal epidural space

Degenerative:	Herniated disc, Hypertrophied ligamentum flavum and facetal arthropathy, Synovial cyst
Infective:	Pyogenic abscess, tuberculous abscess, fungal infection.
Neoplastic: i) Benign ii) Malignant	Lipoma/lipomatosis, angiolipoma, hemangioma, paraspinal arteriovenous malformation/fistula, arachnoid cyst, dermoid, epidermoid cyst Lymphoma, metastases.
Miscellaneous:	Epidural hematoma (spontaneous or post traumatic), Dilated venous plexus in collateral pathway in IVC obstruction, Hirayama's disease

Hypertrophied ligamentum flavum with facetal arthropathy

Ligamentum flavum drapes the posterolateral aspect of the spinal canal. The bulk of ligament comprises elastin fibres (80%) with remainder being collagen—a fact that contributes to an increased signal on T1W compared to other ligamentous structures in the body. With aging, the ratio of fibres reverses decreasing the elasticity.[10] Along with disc degeneration and facetal arthrosis, hypertrophy of ligamentum flavum contributes to spinal canal stenosis. The mechanism of hypertrophy is unclear, however, it may occur due to chronic inflammation leading to an accumulation of fibrous tissue with scarring.[11] The thickness of ligamentum flavum increases with age and is more pronounced in the lower lumbar levels due to higher mechanical stress.[12] Occasionally, calcium pyrophosphate dehydrate may deposit in the ligamentum flavum that appears hypointense on all sequences on MRI and shows calcification on Computed Tomography (CT) [Figures 5 and 6].

The normal facet joint is characterized by a uniform joint space of 2–4 mm, with no osteophytosis or subchondral bone reaction. Based on CT and MRI findings, Weishaupt *et al*.[13] graded facetal arthropathy as:

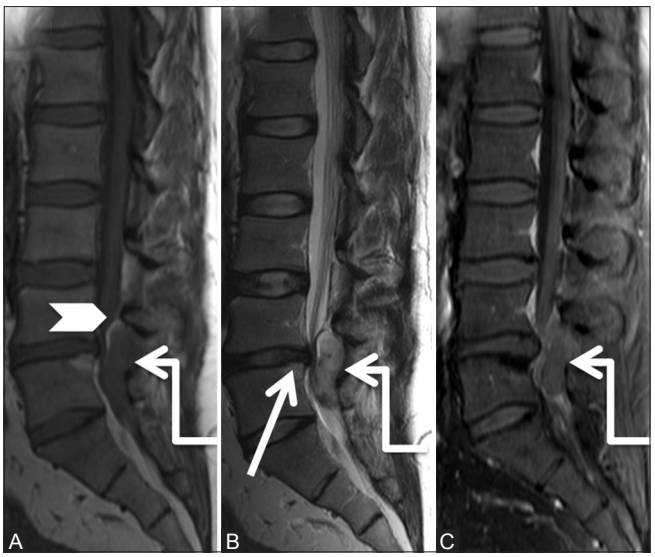

Figure 3a (A-C): Degenerative: Herniated disc: 37-year-old male with severe left leg radiating pain. Sagittal T1-weighted (A), T2-weighted (B) and Post-contrast T1 fat saturated (C) images of lumbar spine showing disc protrusion at L4-5 level (arrow). Note soft tissue signal intensity lesion (elbow arrow) in the posterior epidural space appearing hypointense on T1, hyperintense on T2 and showing peripheral rim enhancement. Compressed posterior epidural fat is seen displaced superiorly and anteriorly (arrowhead)

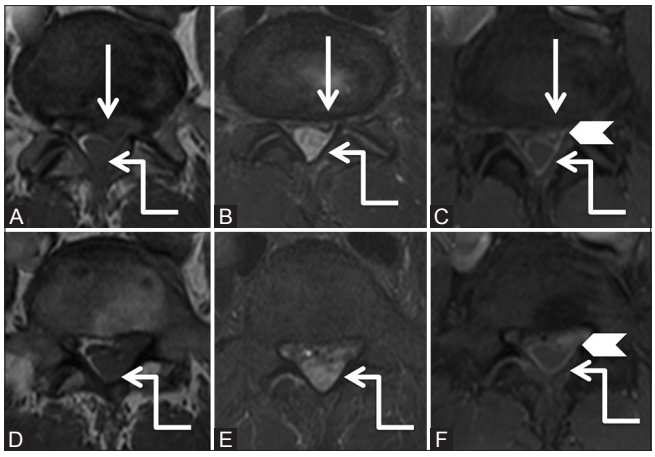

Figure 3b (A-F): Degenerative: Herniated disc: Axial T1-weighted (A, B), T2-weighted (C, D) and post-contrast T1 fat saturated (E, F) images at the level of disc (proximal row) and a level inferior to it (distal row) show diffuse disc bulge with left paracentral extrusion (arrow). Note tract-like enhancement (arrowhead) extending from the disc to peripherally enhancing soft tissue lesion in the posterior epidural space (elbow arrow) suggestive of disc herniation

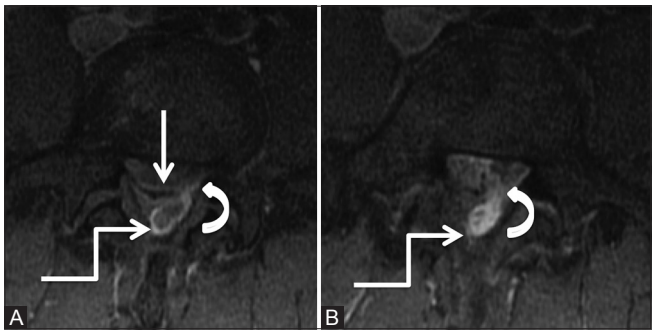

Figure 4b (A and B): Degenerative: Herniated disc: Axial post contrast T1 fat-saturated images of lumbar spine at the level of disc and a level below it, showing posterior protrusion with left paracentral extrusion of disc (arrow). Tract-like enhancement (curved arrow) is seen extending from the disc to heterogeneously enhancing soft tissue in the posterior epidural space (elbow arrow) suggestive of herniated disc. [Courtesy: Dr Vipul Chemburkar]

Grade 1 or Mild osteoarthritis: Shows narrowing of the facet joint space (<2 mm) and/or small osteophytes, and/or mild articular process hypertrophy.

Grade 2 or Moderate osteoarthritis: Shows narrowing of the facet joint space (<2 mm) and/or moderate osteophytes, and/or moderate articular process hypertrophy and/or mild subarticular bone reaction (erosions).

Grade 3 or Severe osteoarthritis: Shows narrowing of the facet joint space (<2 mm) and/or large osteophytes, and/or large articular process hypertrophy, and/or severe subarticular bone reaction (erosions and/or cysts).

Synovial cysts

Synovial cyst represents protrusion of synovial membrane from degenerated facet joints into the spinal canal[14]

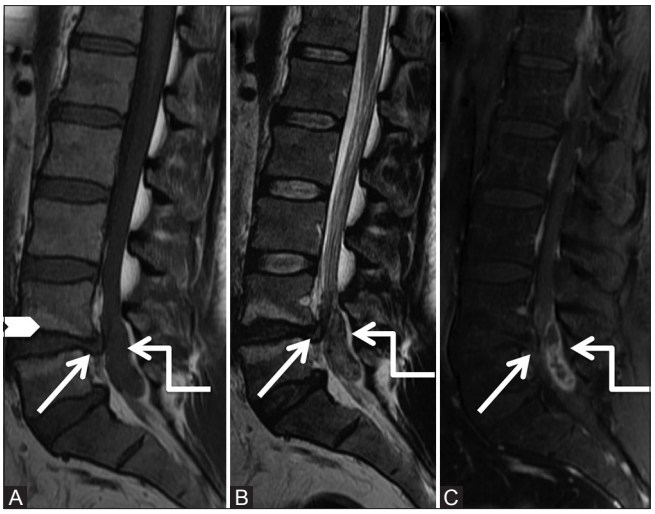

Figure 4a (A-C): Degenerative: Herniated disc: Sagittal T1-weighted (A), T2-weighted (B) and post-contrast T1-weighted fat saturated (C) images of lumbar spine showing posterior protrusion of L4-5 disc with posterior osteophyte (arrow) along with elongated posterior epidural soft tissue lesion (elbow arrow), which appears isointense on T1-weighted and heterogeneously hyperintense on T2-weighted and peripheral rim enhancement, causing severe canal stenosis. Note Type II fatty Modic degenerative changes at L4-5 end plates (arrowhead)

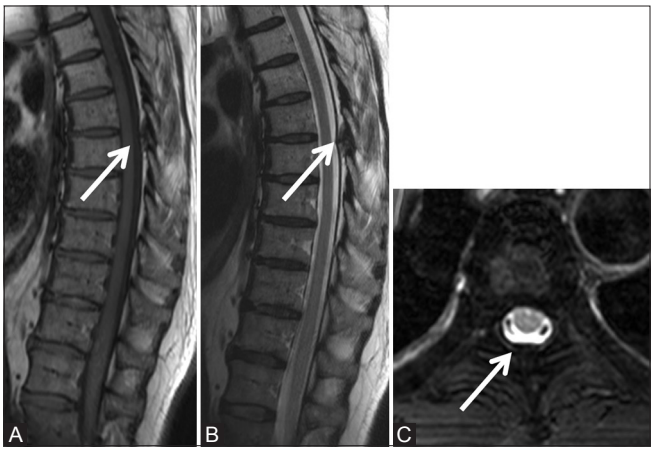

Figure 5 (A-C): Degenerative: Hypertrophied ligamentum flavum: Sagittal T1-weighted (A), T2-weighted (B), and axial T2 fat saturated (C) images of thoracic spine in a 62-year-old male with a known carcinoma of the lung with backache, showing focal hypertrophy of ligamentum flavum (arrow) at T4-5 level effacing the posterior epidural space. No abnormal vertebral signal or soft tissue noted on axial images

contrary to the ganglion pseudocyst, which represents a cyst that is devoid of synovial lining. Often synovial cysts and ganglion pseudocysts are referred to as juxtafacet cysts. In a review by Bydon *et al*., 96.2% synovial cysts were located in the lumbar (75.4% at the L4–L5 level), 2.6% in the cervical, and only 1.2% in the thoracic spine.[15] These cysts may be associated with disc degeneration and spondylosis. Synovial cysts [Figures 7 and 8] on MRI show T2 hypointense fibrous/calcified capsule with variable internal signal on T1W and T2W images depending on cysts contents.[16] The cysts may show adhesions to the dura mater and nerve roots.

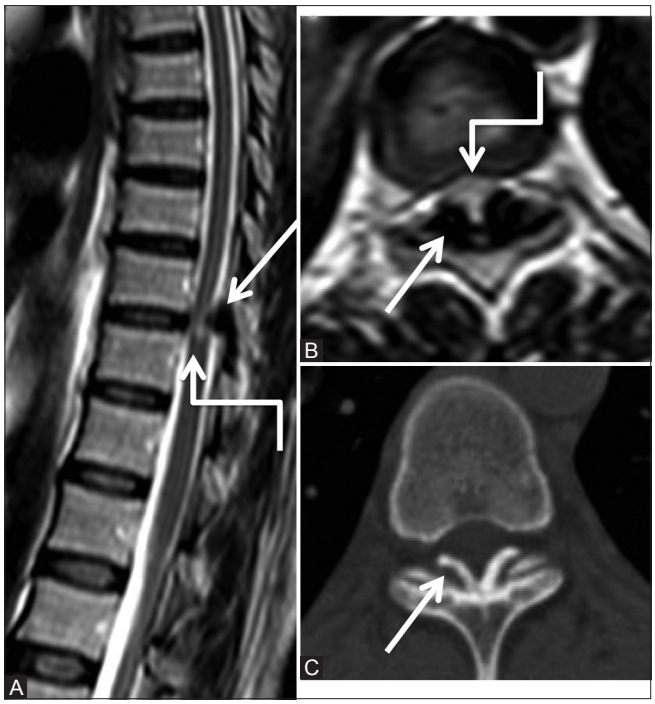

Figure 6 (A-C): Degenerative: Ligamentum flavum calcification: Sagittal (A), axial T2-weighted (B) and computed tomography (CT) axial (C) images of lower thoracic spine in 38-year-old female showing focal thickening of the ligamentum flavum (arrow) at lower thoracic level, which appears hypointense on T2-weighted images and shows calcification on the CT scan. These efface the posterior subarachnoid space and indent on the cord with edema in cord (elbow arrow)

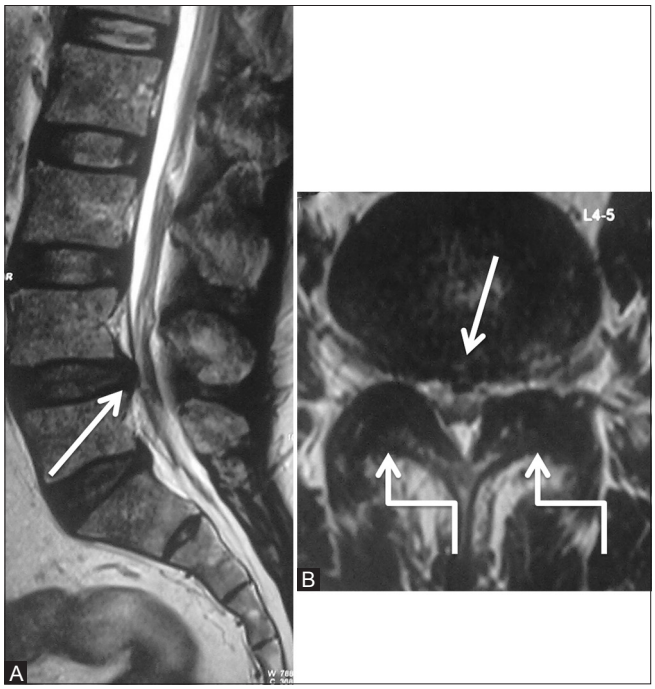

Figure 8a (A and B): Degenerative: Synovial cyst: Preoperative scan: Sagittal (A) and axial (B) T2-weighted images in a 59-year-old male patient with lower limb radiculopathy, showing diffuse disc bulge (arrow) at L4-5 level along with moderate degenerative facetal arthropathy (elbow arrow), causing moderate to severe canal and bilateral lateral recess narrowing. Patient underwent decompressive laminectomy at the L4-5 level

Figure 7 (A and B): Degenerative: Synovial cyst: Magnetic resonance imaging of a 90-year-old female done for left-sided radiculopathy. Parasagittal and axial T2-weighted images show degenerative changes in the lumbar spine at all levels. Note moderate degenerative facetal arthropathy at L4-5 level along with synovial cyst (arrow) from the left facetal joint, causing severe canal and left lateral recess narrowing

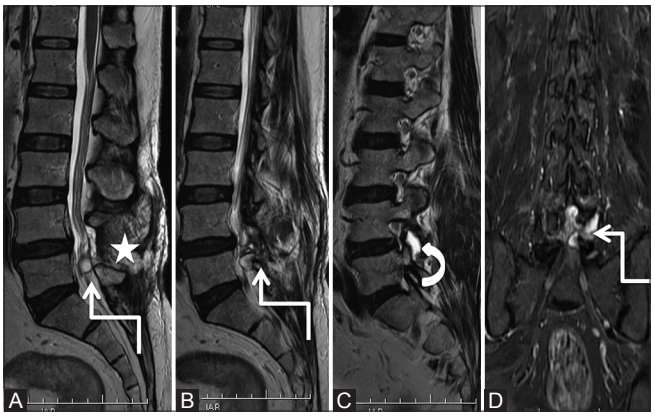

Figure 8b (A-D): Degenerative: Synovial cyst: Postoperative scan at 3 months with patient having left lower limb radiculopathy: Sagittal T2-weighted (A-C) and coronal short T1 inversion recovery (D) images show a well-defined lobulated hyperintense cystic lesion (elbow arrow) in the posterior epidural space at L4-5 level, which communicates with fluid in the left L4-5 facet joint (curved arrow). Note postoperative changes in the paraspinal region (star)

Synovial cyst needs to be differentiated from the ligamentum flavum cyst which arises due to reduced elasticity of ligamentum flavum with continued stress. The latter does not communicate with facetal joints and is more prone to hemorrhage due to rupture of vessels in degenerated ligamentum flavum[17] whereas the former often has a calcified wall. This differentiation is important because synovial cysts occur secondary to facetal arthropathy and require exploration of facet joints.

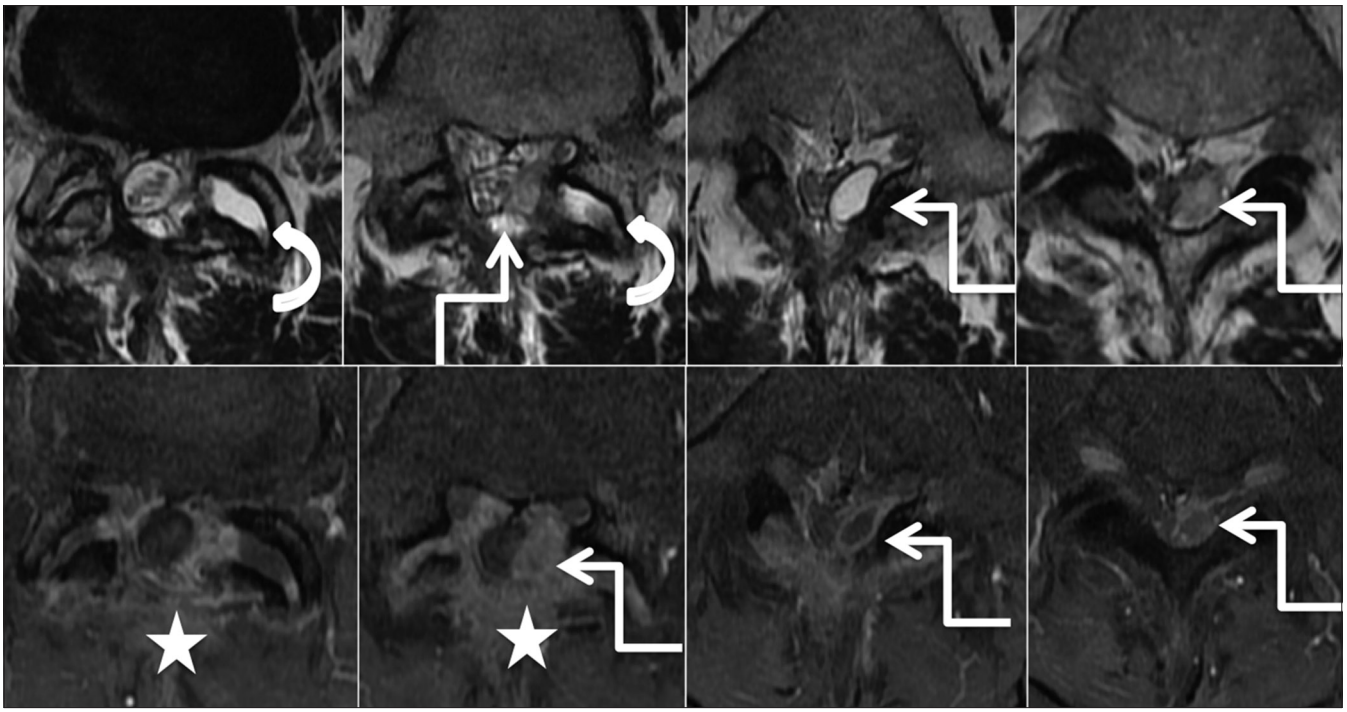

Figure 8c: Degenerative: Synovial cyst: Postoperative scan: Axial T2-weighted (upper row) and post-contrast T1 fat saturated (lower row) images from superior to inferior aspect, show laminectomy defect with postoperative changes in the paraspinal region (star). Fluid in left L4-5 facet joint (curved arrow) appears to communicate with the lobulated cystic lesion showing rim enhancement in the left posterior epidural space. [Courtesy: Dr Vipul Chemburkar]

Synovial cysts can be aspirated under CT or fluoroscopy guidance with/without steroid injection in the epidural or extraforaminal space. However, cysts with gelatinous contents may be nonaspirable and residual cyst capsule may cause persistent compression of nerve roots. These techniques offer short-term benefits with high rate of long-term failures. Surgical decompression and removal of the cyst offers the best outcome.[18] Treatment of the ligamentum flavum cyst is mainly surgical consisting of resection of the cyst and affected ligamentum flavum to decompress the spinal canal and relieve the patient from radiculopathy.

Infective

Pyogenic

Spinal epidural abscess is a rare[19] but serious condition with multiple causes. Primary abscesses occur after spinal trauma, injections, surgery, or after direct introduction of pathogens into the epidural space (e.g., as a complication of vertebral osteomyelitis). Hematogenous dissemination of microbes present elsewhere to the epidural space constitute the secondary type. Patients with diabetes mellitus, acquired immunodeficiency syndrome, or who are under immunosuppressive treatment after organ transplantation, drug addiction, alcoholism, cancer, and systemic inflammation or infection are more susceptible for contracting secondary epidural abscess.[20,21] The most common pathogen in both forms is *Staphylococcus aureus*,[22,23] with methicillin-resistant *Staphylococcus aureus* being increasingly isolated.

The abscess extends laterally and vertically in the epidural space and may occasionally involve the whole length of the spinal canal. Most epidural abscesses are located at the thoracic or lumbar level because the epidural space is larger in these areas.[24] In adults, they are predominantly located anteriorly, whereas a posterior location is more common in children. Moreover, in children, these abscesses tend to be more extensive.[25] Restricted diffusion on MRI confirms the presence of a pyogenic abscess [Figure 9]. The main determinant of outcome for patients with a spinal epidural abscess is the neurologic status at the time of diagnosis.[23] Combined surgical drainage and prolonged antibiotic therapy remain the ideal treatment.

Tuberculosis

Spinal tuberculosis (TB) accounts for 2% of all cases of TB, 15% of extrapulmonary TB, and 50% of all cases of skeletal TB.[26] It is caused by hematogenous spread of *Mycobacterium tuberculosis* from primary focus in lung, lymph node, or gastrointestinal tract.[27]

Spinal tuberculosis classically affects the discovertebral region with involvement of two contiguous vertebral bodies and destruction of intervening disc (spondylodiscitis), however, several vertebrae, skip lesions, or single vertebral body may be involved. It may be associated with paravertebral, subligamentous, or anterior epidural soft tissue/abscess. Dorsolumbar region is the most commonly

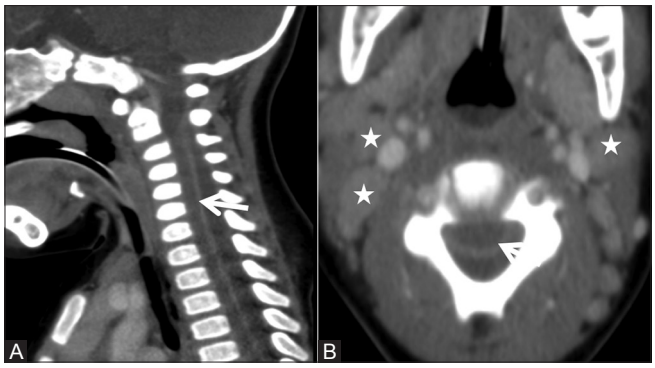

Figure 9a (A and B): Infective: Pyogenic abscess: Sagittal (A) and axial (B) Computed tomography scan showing hypodense fluid collection in the posterior epidural space with compression of cord anteriorly. Thick enhancing dura is also seen (arrow). Few enlarged cervical nodes are seen (asterisk)

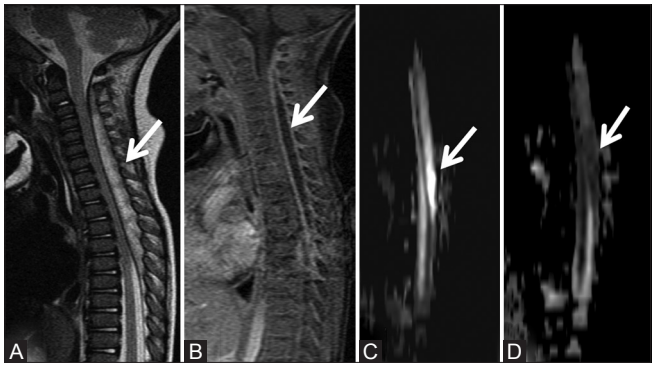

Figure 9c (A-D): Infective: Pyogenic abscess: Sagittal T2-weighted (A) and post-contrast (B) images showing the extent of abscess from C2 to T7 level. The cervical and upper thoracic cord is compressed anteriorly, however, its signal intensity is normal. The osseous elements are normal. No evidence of osteomyelitis is seen. Diffusion weighted image (C) shows hyperintense signal (arrow), which is hypointense on the apparent diffusion coefficient map (D). Group A streptococci were isolated from the pus

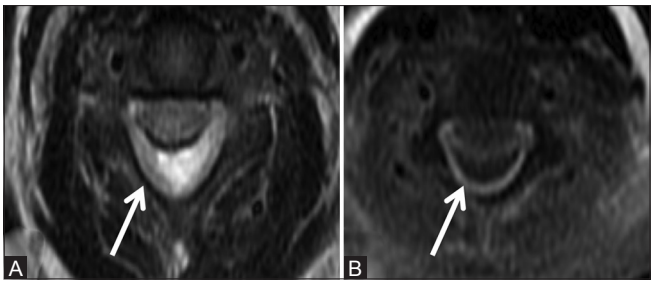

Figure 9b (A and B): Infective: Pyogenic abscess: Axial T2-weighted image (A) shows hyperintense collection (arrow) in the posterior epidural space, which shows peripheral enhancement on post-contrast axial image (B)

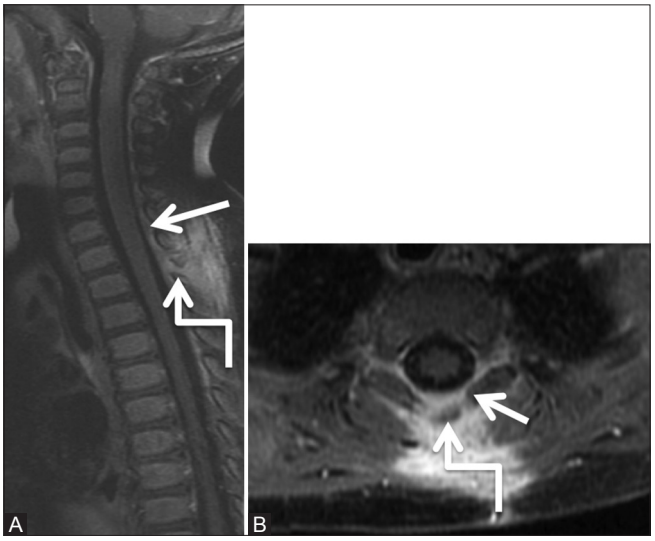

Figure 9d (A and B): Infective: Pyogenic abscess: Follow-up scan 6 weeks post-decompressive laminectomy and course of antibiotics: Post-contrast T1-weighted Sagittal (A) and axial (B) images show complete resolution of abscess. Minimal dural enhancement is seen (arrow). Note laminectomy defect at T1-2 level (elbow arrow)

affected.[28] Occasionally, isolated involvement of the neural arch or posterior elements may be seen. MRI findings include erosion of lamina, posterior epidural soft tissue/abscess, and pyomyositis along the posterior spinal muscles. The posterior epidural soft tissue/abscess may compress upon the spinal cord and spastic lower limb weakness may ensue [Figures 10-12]. Pateints with neurological deficits need emergent decompressive laminectomy.[29]

Neoplastic: Benign

Spinal epidural lipomatosis

Spinal epidural lipomatosis is characterised by pathological accumulation of unencapsulated adipose tissue in the extradural space.[30] It occurs with prolonged steroid use, Cushing's syndrome, or morbid obesity. In idiopathic form, epidural fat deposition is also seen in nonobese patients.[31] Clinical symptoms depend on the level of vertebral involvement and disease severity. Usually, it occurs in the thoracic region in the dorsal epidural space. Backpain is the most common symptom. Other manifestations include insidiously progressive sensory and motor symptoms. Involvement of the thoracic spine may result in myelopathic symptoms.

MRI is the imaging modality of choice to assess the extradural fat as well as compression on cord and nerve roots. Epidural lipomatosis is chararcterized by hyperintense signal both on T1W and T2W images, which is supressed on fat-saturated images. The lesion causes circumferential compression of the dural sac [Figures 13-16]. In the lumbar canal, the dural sac appears geometric, polygonal, spiculated and Y-shaped due to the variable presence of meningovertebral ligaments epidural space anchoring the dura mater with the osteofibrous walls of the lumbar canal.[32] Epidural fat thickness greater than 7 mm is diagnostic of spinal epidural lipomatosis [Figure 15].[31] Treatment depends on the severity of symptoms. Decompressive laminectomy is needed with resection of epidural lipomatosis in patients with neurodeficits. Weight reduction, treatment

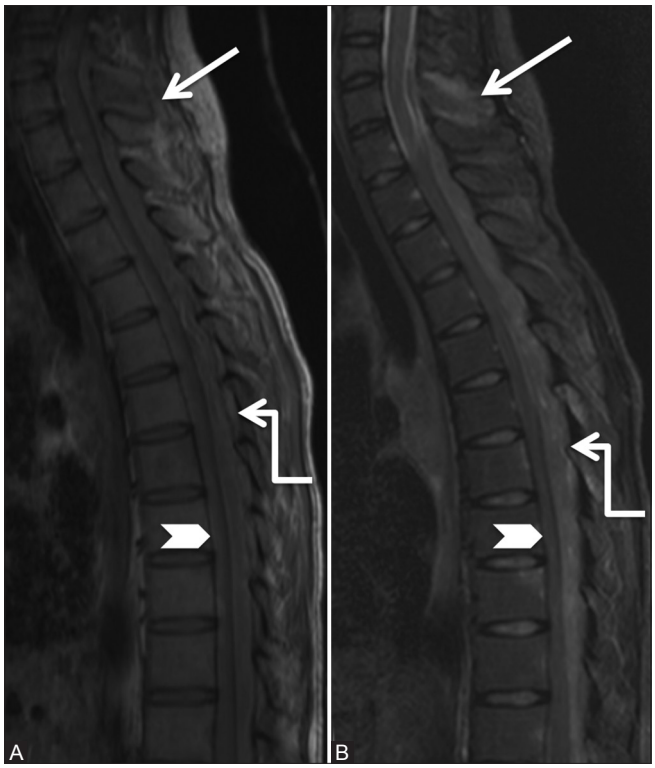

Figure 10a (A and B): Infective: Tuberculosis: 19-year-old female with backache and cough. Sagittal T1-weighted (A) and short T1 inversion recovery (B) images of cervicothoracic spine showing abnormal signal in C7 spinous process (arrowhead) with surrounding soft tissue. Note large posterior epidural abscess (elbow arrow) extending from C7 to T12 levels, compressing the cord anteriorly (arrowhead)

for Cushing's syndrome, and weaning and stoppage of exogenous steroids constitute conservative therapy.[33]

Lipomyelocele [Figure 16] and lipomeningocele are closed types of spinal dysraphism, which are characterized by the presence of neural placode and hypertrophy of subcutaneous fat which extends through the posterior dural defect into the spinal canal (extradural as well as intradural). Lipomyelocele have neural placode–lipoma interface in the spinal canal or at its edge as compared to lipomeningocele, where the interface is outside the spinal canal. Lipomyelomeningocele is also associated with enlargement of anterior cerebrospinal fluid (CSF) subarachnoid spaces.[34]

Spinal angiolipoma

Spinal angiolipoma is a rare, benign lesion that contains mature adipose and vascular elements, is usually noninfiltrating, and occurs in the posterior epidural space.[35] Infiltrating spinal angiolipoma, however, has a tendency to invade adjacent structures including vertebral bodies and may extend beyond the neural foramen.[35,36] Contrast-enhanced MRI is the best modality to diagnose these lesions as well as to differentiate spinal angiolipoma from epidural lipomatosis. On MRI, Hu *et al*.[37] divided spinal angiolipoma into two types based on the ratio of fat to vessels.

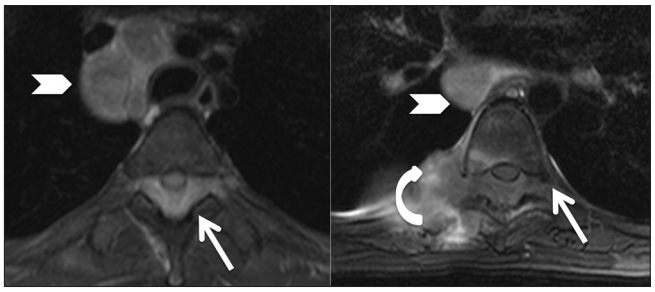

Figure 10b: Infective: Tuberculosis: Axial T2-weighted images at upper and lower thoracic levels, showing large posterior epidural abscess (arrow) compressing the cord anteriorly and extending into both the intervertebral foramina. Right costotransverse joint is involved with adjacent soft tissue (curved arrow). Enlarged mediastinal nodes are seen (arrowhead)

Type 1: These lesions are predominantly fatty, and hence appear hyperintense on T1W and T2W images. Blood vessels within the lesion appear as T1 hypointense strips or spots, which show post-contrast enhancement.

Type 2: Vascular component forms more than 50% of the lesion and is surrounded by fat. These may appear heterogenous on T1W and T2W images and most of the lesion shows intense enhancement.

Absence of flow voids in spinal angiolipoma distinguishes them from high flow arteriovenous malformations and capillary hemangiomas. In addition, the margins of capillary hemangioma with adjacent fat (which is not part of tumor) are clear as compared to spinal angiolipoma whose fat and vascular interface is irregular and vague.[38] Surgical removal of the lesion to decompress the cord is necessary.

Hemangioma

Spinal epidural hemangiomas are rare and are classified into arteriovenous, cavernous, capillary, or venous depending upon the predominant type of vascular channel.[39] They are categorized into 4 types:

Type A: Cyst-like mass that shows hyperintense signal on T1W images (arteriovenous hemangioma)

Type B: Cyst-like mass with isointense signal on T1W images (venous type hemangioma)

Type C: A solid hypervascular mass that reveals homogenous hyperintense signal on T2W and intense post-contrast enhancement (cavernous type)

Type D: An epidural hematoma that shows high signal on T1 and very low signal on T2W images (cavernous type with hematoma).

A T2 hypointense rim around the hemangioma may be a result of fibrous capsule, interface between mass and adjacent

Figure 10c: Infective: Tuberculosis: Follow-up scan after thoracic laminectomy and on anti-tuberculous treatment. Magnetic resonance imaging scan 2 months later shows increase in the posterior epidural soft tissue with necrosis (elbow arrow). Persistent compression on spinal cord (arrowhead) is seen. Note the persistent abnormal signal C7 spinous process (arrow)

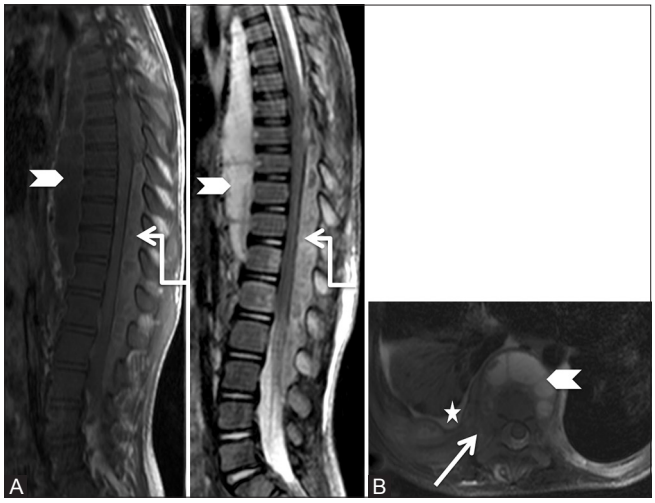

Figure 11 (A and B): Infective: Tuberculosis: 7-year-old boy with paraparesis. Sagittal T1-weighted (A) and T2-weighted (B) images of spine showing large posterior epidural abscess (elbow arrow) extending from T6 to L3 levels, compressing the cord anteriorly. Also note large prevertebral soft tissue (arrowhead). On axial T2 fat-saturated images, involvement of right costotransverse and costovertebral junction and adjacent rib (arrow) is seen. Minimal right pleural effusion is seen (star)

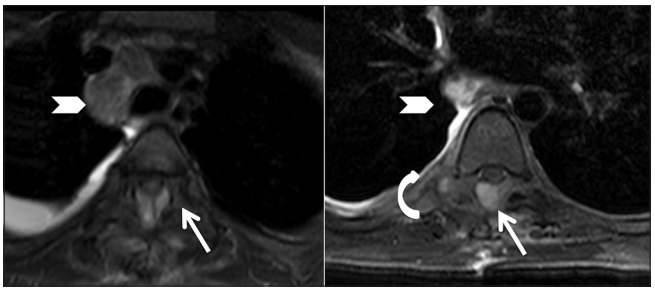

Figure 10d: Infective: Tuberculosis: Follow-up scan after thoracic laminectomy and on anti-tuberculous treatment: Axial T2 fat-saturated images showing posterior epidural abscess (arrow) compressing the cord. Persistent abnormal signal is seen in right costotransverse joint associated with much lesser amount of soft tissue (curved arrow). Also note the decrease in the size of mediastinal nodes (arrowhead)

Figure 12a (A and B): Infective: Tuberculosis: 30-year-old male with backache. Sagittal T1-weighted (A) and T2-weighted (B) images of thoracic spine showing abnormal signal in the posterior half of T8 vertebral body and in spinous processes of T7 and T8 vertebrae (arrows). Localized posterior epidural abscess (elbow arrow) at T7-8 level is seen compressing the cord with edema in cord

posterior longitudinal liagament and duramater, chemical shift artifact between epidural fat and intratumoural fluid content, and staining due to hemosiderin.[39]

Paravertebral arteriovenous malformations/fistulas

Arteriovenous malformations of spine are classified as spinal cord arteriovenous malformation, spinal cord arteriovenous

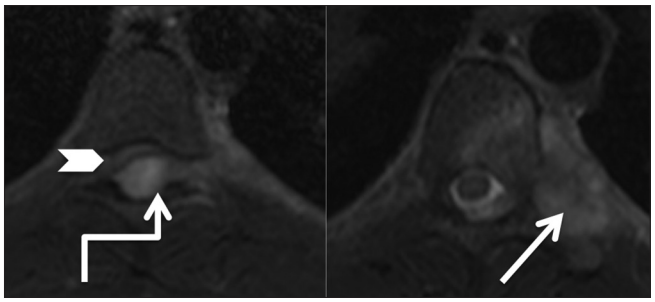

Figure 12b: Infective: Tuberculosis: Axial T2-weighted images of thoracic spine at T7-8 level showing posterior epidural abscess (elbow arrow) compressing the cord anteriorly (arrowhead) with edema in cord. Note the involvement of left costotransverse and costovertebral joint (arrow)

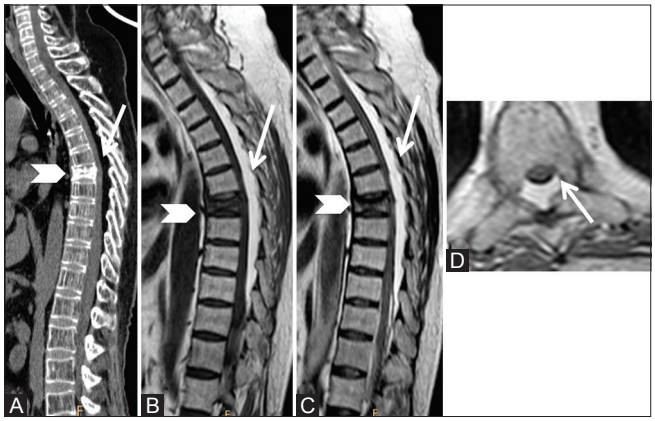

Figure 14 (A-D): Benign lesions: Spinal Epidural lipomatosis: 48-year-old male on long-term steroids. Sagittal computed tomography scan (A), T1-weighted (B), T2-weighted (C), and axial T2-weighted (D) images showing excessive proliferation of posterior epidural fat (arrow) in thoracic region. Note the prominence of trabeculae and fatty marrow in vertebrae suggestive of osteoporosis. Old compression fracture of T6 vertebral body (arrowhead) is also seen

fistula, dural arteriovenous fistula, and arteriovenous malformations occuring outside the dura with drainage into the epidural veins. The last group is called as paravertebral arteriovenous malformations/fistulas (PAVM/PAVF).[40]

A paraspinal arteriovenous fistula (AVF) is a rare subtype of spinal AVF which also comprises intracanalicular and vertebral AVFs.[41] A paraspinal AVF is most commonly described in the cervical region, with possible etiology being traumatic or congenital.[41,42] The lesion is fed by muscular or vertebral branches and drainage may be via ectatic paravertebral, epidural. or intradural veins.

The presentation of these lesions is variable. It may present as a pulsatile subcutaneous mass in the paravertebral musculature; dysphagia, if in the cervical region or with venous congestion myelopathy characterized by dilated perimedullary veins with central cord edema or compressive myelopathy due to mass effect from dilated epidural veins or with bruit. A paraspinal AVF with a high flow may even present as congestive heart failure. A paraspinal AVF is

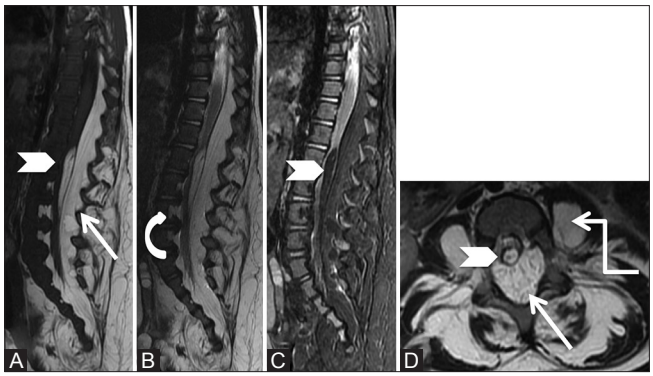

Figure 13 (A-D): Benign lesions: Lipomatosis: Sagittal T1-weighted (A), T2-weighted (B), T2 fat saturated (C), and axial T2-weighted (D) images of lumbar spine in a 11-month-old female showing excessive fat in the posterior epidural space (arrow), which also extends laterally and causes scalloping of vertebral bodies (curved arrow). It is associated with filum terminale lipoma (arrowhead). Also note lipomatous tissue in both paraspinal and psoas muscles (elbow arrow)

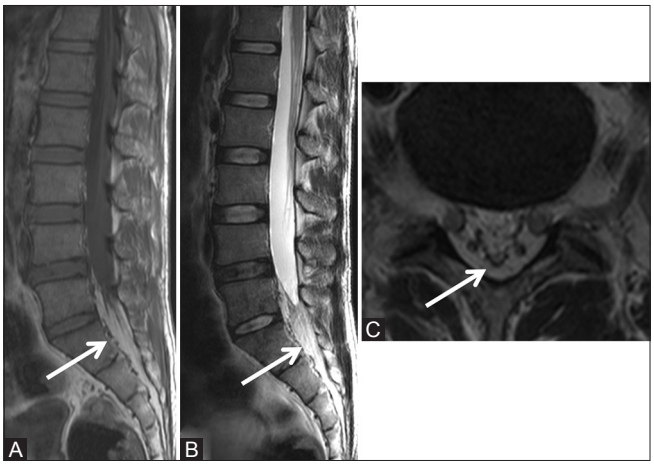

Figure 15 (A-C): Benign lesions: Epidural Lipomatosis: 36-year-old female with low backache. Sagittal T1-weighted (A), T2-weighted, (B) and axial T2-weighted (C) images showing excessive proliferation of epidural fat (arrow) below L5 level resulting in the deformation of thecal sac with its narrowing

unique in terms of its relentless progression and challenges in diagnosis and management.[41]

Imaging depicts the vascular malformation, cord changes, and pressure erosions on vertebrae.[42] Additional dilated paravertebral vascular channels may be seen [Figure 17]. Cobb syndrome is characterized by coexistence of intramedullary AVM and PAVM. Diagnostic angiography helps in evaluating the site of shunt, arterial supply, and venous drainage of these lesions.

Endovascular embolization is the definitive management of the pathology.[41]

Arachnoid cyst

Spinal extradural arachnoid cysts are a relatively rare cause of compressive myelopathy.[43] They have been

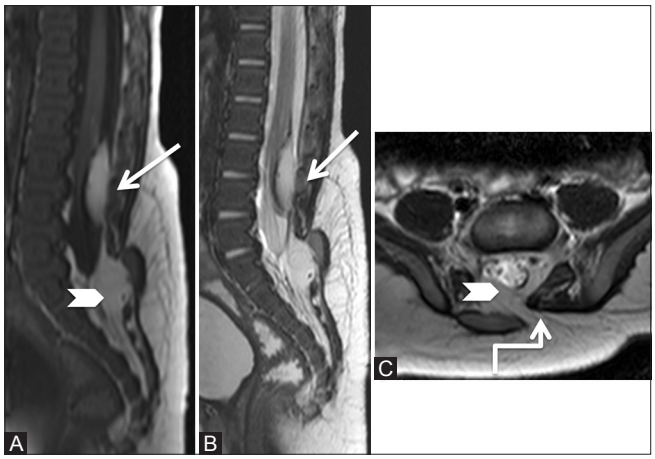

Figure 16 (A-C): Benign lesions: Lipoma: 3-month-old male child had a soft swelling over the lower back since birth. Sagittal T1-weighted (A), T2-weighted (B), and axial T2-weighted (C) images showing low lying conus at L3-4 level with intradural lipoma (arrow) adherent to the posterior surface of cord. Spina bifida is seen at S1 level (elbow arrow), and through it, the subcutaneous fat extends into the epidural space (arrowhead). These findings are suggestive of lipomyelocele

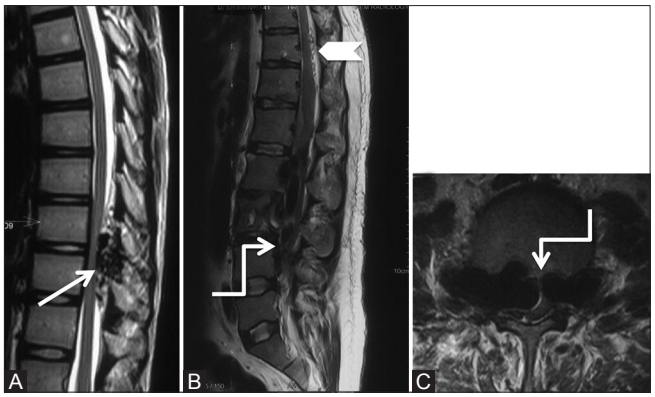

Figure 17 (A-C): Benign: Paraspinal Artervenous Fistula: 26-year-old male with a history of low backache and paraparesis. Sagittal T2-weighted image at lower thoracic (A), Sagittal (B), and axial images (C) through the lumbar spine show presence of multiple flow voids (arrows) in the posterior epidural space in lower thoracic region, displacing the thoracic cord anteriorly. Multiple flow voids are also seen on the surface of cord due to dilated perimedullary veins (arrowhead). Massively dilated anterior epidural venous plexus and intervertebral veins (elbow arrow) are seen compressing the cauda equina and scalloping the lumbar vertebral bodies

reported at all locations, however, most commonly seen at middle to lower thoracic regions, posteriorly. There is protrusion of arachnoid membrane herniating through a dural defect resulting in communication with the intradural subarachnoid space. The exact etiology of these cysts is still unclear, these include congenital or acquired from trauma, arachnoiditis, infection, inflammation, or iatrogenic cause. These cysts enlarge from CSF accumulation and cause symptoms due to compression on the spinal cord or nerve roots.[44]

MRI is the modality of choice for diagnosing arachnoid cysts. It shows a cystic lesion following CSF signal intensity, with variable compression on the spinal cord and nerve roots. On T1W images, epidural fat capping of the lesion at superior and inferior aspect of the cyst confirms extradural location. Long standing lesions may cause vertebral body scalloping, neural foraminal widening and expansion, erosion of pedicles, and widening of interpedicular distance [Figure 18]. CT myelography shows communication of the cyst with the subarachnoid space.[43]

Nabor *et al.*[45] classified spinal meningeal cysts into three categories:

1) Type 1: Extradural meningeal cyst without spinal nerve root fibres;
   Type 1 meningeal cysts consist of extradural arachnoid cysts (type Ia) and sacral meningoceles (type Ib).
2) Type 2: Extradural meningeal cyst with spinal nerve root fibres
3) Type 3: Intradural meningeal cyst.

Treatment for symptomatic cysts is the surgical excision of the lesion with repair of the dural defect. Complete excision of the cysts involves long-level laminectomy with its complications, and hence currently, tailored laminotomy with cyst fenestration and dural repair is favored.[44,46]

Neoplastic: Malignant lesions

Lymphoma

Spinal lymphomas are divided into three types based on location and growth pattern. These are paraspinal, vertebral, and epidural.[47]

Bone marrow involvement in lymphoma can be focal or diffuse and indicates stage IV disease. Abnormal marrow appears hypointense on T1W and hyperintense on T2 fat-saturated and short T1 inversion recovery (STIR) sequences. There may be multifocal lesions, cortical destruction, and associated soft tissue masses [Figure 19].

Primary spinal epidural lymphoma is much less common and there are no other recongnizable sites of disease at the time of diagnosis.[48]

Thoracic spine is most commonly involved due to its greater length, enhanced ability to accommodate bulky diseases in the thorax and abdomen, and due to rich venous plexus. Symptoms occur due to spinal cord and nerve root compression.

MRI of the whole spine and brain are recommended to determine the complete extent of the disease. The epidural soft tissue appears hypointense-to-isointense to cord on T1W and isointense to hyperintense on T2W images with intense homogenous enhancement. The tumor has infiltrative pattern and may extent into the neural foramina. Spinal cord compression may be seen.

Figure 18a (A and B): Benign lesions: Arachnoid cyst: Sagittal T1-weighted (A) and T2-weighted (B) images in a 72-year-old female, with long standing back ache, show a well-defined cerebrospinal fluid signal intensity lesion (arrow) in the posterior epidural space extending from T10 to L1 levels. The lesion effaces posterior epidural fat and shows mass effect on the spinal cord, which is displaced anteriorly

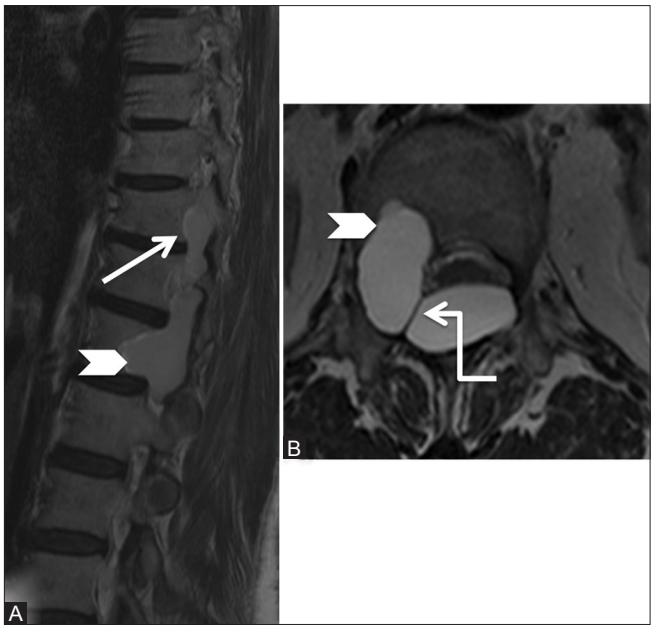

Figure 18b (A and B): Benign lesions: Arachnoid cyst: Parasagittal (A) and axial (B) T2-weighted images showing arachnoid cyst (arrow) extending from the posterior epidural space into the intervertebral foramina and causing scalloping of posterior vertebral body on the right side (arrowhead). Note the meningovertebral ligament traversing the lesion (elbow arrow)

Primary spinal epidural lymphoma may occur due to hematogenous spread from unidentified lymphoid sources or from direct spread from vertebral bodies or from contiguous spread from paravertebral region through neural foramina. Histologically, primary spinal epidural lymphoma is commonly of Non-Hodgkin's type than Hodgkin's type.[49]

Metastases

Spine is the most common osseous site for metastases[50] and third most common after lung and liver metastases. Metastases can involve the vertebrae, epidural space, leptomeninges, or the spinal cord.[51]

Breast, prostate, thyroid, kidney, and lung cancers are common primary tumors associated with bone metastases.

Focal bony lesions appear hypointense on T1W and hyperintense on T2W images. Occasionally, rim of T2 hyperintense signal is seen around the lesion, the halo sign. However, sclerotic lesions appear hypointense on all sequences. Diffuse abnormal marrow signal may be observed. Post-contrast T1 fat-saturated images delineate the enhancing metastases as well as associated paraspinal and epidural soft tissue. Epidural soft tissue is commonly associated with the destruction of vertebrae and direct extension throught posterior longitudinal ligamant, or extension through the intervertebral foramina or hematogenous or lymphatic spread. Epidural soft tissue results in the compression of thecal sac and its contents, i.e., spinal cord and nerve roots. Posterior elements, especially the pedicles, may be involved by metastases [Figures 20 and 21].

Miscellaneous

Epidural hematoma

Spinal epidural hematoma is a rare condition and could be either post-traumatic or spontaneous. It presents as an acute onset of back pain and symptoms due to compression on the spinal cord and cauda equina. Predisposing factors include coagulopathy, anticoagulation, therapeutic thrombolysis, vascular anomaly, disk herniation, Paget disease of bone, Valsalva maneuver, neoplasms, infections, and minor vertebral trauma. The source of hemorrhage is attributed to valveless epidural venous plexus.[52,53]

MRI is the imaging modality of choice in diagnosing spinal epidural hematoma. Cervical or cervicothoracic locations are most common with extension over multiple levels. Spontaneous spinal epidural hematoma [Figures 22 and 23] usually occurs in the posterior epidural space, whereas traumatic epidural hematomas can occur anteriorly or posteriorly, with the former associated with vertebral body fracture. Post-traumatic spinal epidural hematoma [Figure 24] are often associated with vertebral disease such as rheumatoid arthritis or ankylosing spondylitis in elderly patients. In children, spinal epidural hematoma may occur, without any fracture or dislocation

of the spine.[54] Post lumbar puncture epidural hematoma, though rare, is a known complication.[55]

Spinal epidural hematoma appears biconvex in shape with well-defined borders that taper superiorly and inferiorly. These show variable signal (iso to hyperintense) on T1W images and appear heterogeneously hyperintense on T2W images with hypointense foci. Gradient echo/susceptibility weighted images confirm the presence of hemorrhage [Figures 22-24]. These show mainly peripheral enhancement, however, mixed central and peripheral enhancement and internal septations may be seen. Central enhancement is rare though reported in few cases of spontaneous spinal epidural hematoma,[56] other differentials of tumor, aneurysm, and vascular malformations should be considered. Variable degrees of cord compression may be observed which dictates further management of these patients—urgent decompressive surgery or conservation and observation.

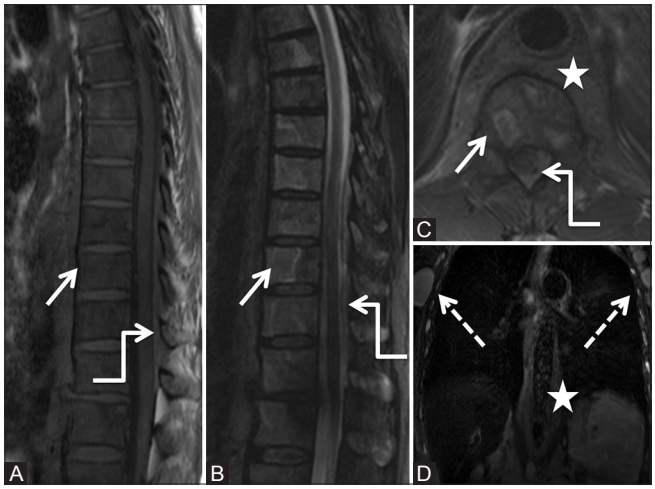

Figure 19 (A-D): Malignant: Lymphoma: 60-year-old male with back pain. Sagittal T1 (A), short T1 inversion recovery (STIR) (B), axial T2-weighted (C), and Coronal STIR (D) images of the thoracic spine show abnormal marrow signal appearing hypointense on T1-weighted images and heterogeneous with focal hyperintense lesions on STIR images in vertebral bodies (arrow) as well as spinous processes. Large paravertebral soft tissue (star) is seen with extension into posterior epidural space (elbow arrow) and causing compression of spinal cord. Note enlarged bilateral axillary lymphadenopathy (dashed arrows). Biopsy was suggestive of non- Hodgkin's lymphoma

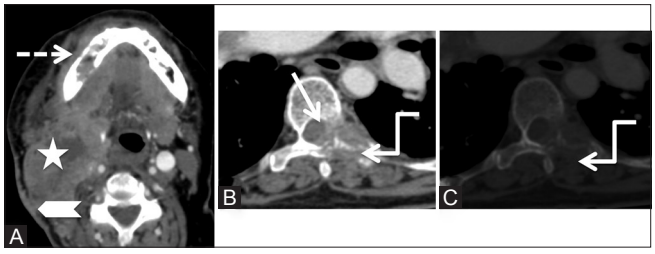

Figure 21 (A-C): Metastases: Post-contrast axial computed tomography scan images at the level of base tongue (A) and lower dorsal spine in soft tissue (B) and bone windows (C), in a 60-year-old female with previous right hemiglossectomy and nodal dissection, show a large heterogeneously enhancing recurrent mass (star) in the right side of the neck extending from submandibular region to posterior triangle. Note the involvement of sternomastoid muscle and overlying skin of the neck (arrowhead). Erosion of the right lower alveolus is also seen (dashed arrow). Lytic lesion is seen in the left transverse process and costotransverse joint (elbow arrow) with posterior epidural soft tissue (arrow) compressing the cord in lower dorsal vertebra

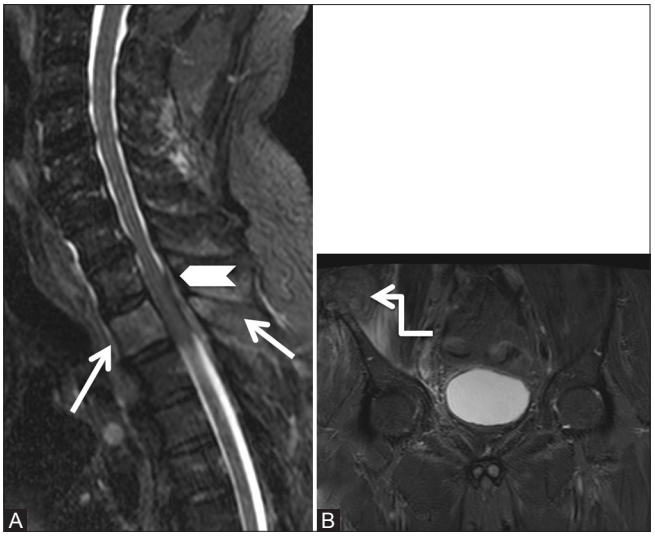

Figure 20 (A and B): Malignant: Metastases: 62-year-old male, a known carcinoma lung patient presented with severe backache. Sagittal short T1 inversion recovery images of cervicothoracic spine (A) and pelvis (B) show abnormal hyperintense marrow signal in T2 vertebral body including its spinous process (arrows). Also seen is posterior epidural soft tissue (arrowhead) compressing the spinal cord. Note large soft tissue lesion with involvement of the right iliac crest by metastatic deposit (elbow arrow)

Figure 22a (A-C): Miscellaneous: Spontaneous epidural hematoma: 65-year-old female with acute onset of severe pain in the cervicodorsal region with weakness in the right lower limb that recovered in 2 days. Sagittal T1-weighted (A), T2-weighted (B), and post-contrast T1 fat saturated (C) images showing lesion in posterior epidural space in cervicothoracic region, appearing hypointense on T1-weighted, heterogeneously hypointense on T2-weighted, and showing minimal peripheral enhancement (arrow)

Collateral pathway in Inferior Vena Cava obstruction

Inferior vena cava (IVC) is the largest venous channel receiving blood from the lower extremities, abdominal, and pelvic viscera and returning to right atrium.

Inferior vena cava obstruction can occur due to thrombus secondary to superior extension of thrombophlebitis in lower extremity or pelvic veins and generalized body conditions such as dehydration, sepsis, coagulopathy, or trauma. Thrombus in IVC is often seen with renal cell carcinoma, more commonly on the right side due to shorter length of right renal vein, Wilm's tumor, adrenal carcinomas or pheochromocytoma, hepatic and pancreatic cancers, and metastatic retroperitoneal adenopathy.

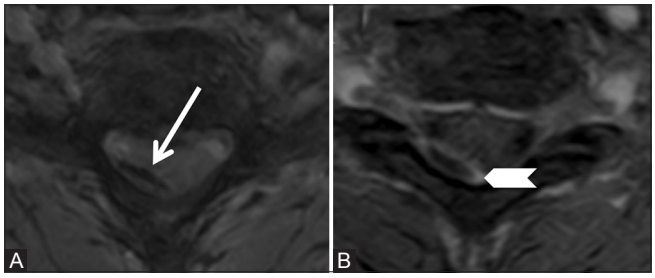

Figure 22b (A and B): Miscellaneous: Spontaneous epidural hematoma: Axial gradient recalled echo (GRE) (A) and post-contrast T1 fat saturated (B) images showing convexoconcave-shaped collection in posterior epidural space on the right side. Blooming is seen on GRE image (arrow). The collection shows peripheral rim enhancement (arrowhead)

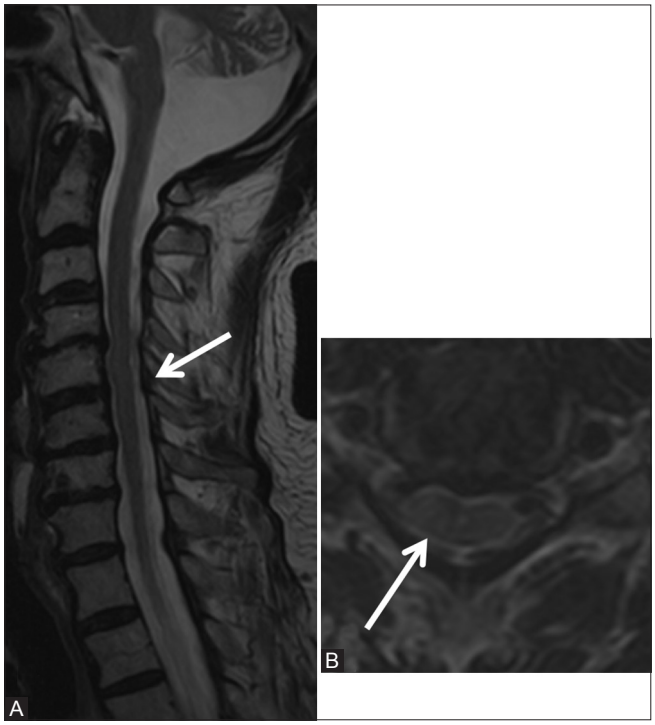

Figure 23b (A and B): Miscellaneous: Spontaneous epidural hematoma: Follow-up scan after 3 months. Sagittal (A) and axial (B) T2-weighted images show complete resolution of the posterior epidural hematoma (arrow)

Enlarged retroperitoneal lymphadenopathy due to tuberculosis, lymphoma, or metastases or hepatic, adrenal, renal, and pancreatic tumors or other retroperitoneal disease may also cause extrinsic compression on IVC.[57]

There are numerous collateral pathways returning the blood from lower extremities and pelvis to right side of

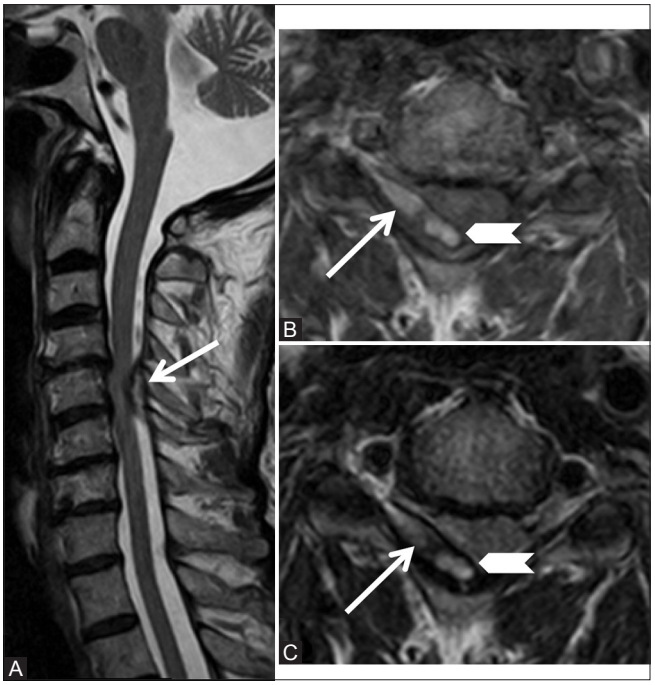

Figure 23a (A-C): Miscellaneous: Spontaneous epidural hematoma: 72-year-old male complained of acute onset neck pain since 10 days with development of right upper and lower limb weakness. Sagittal T2-weighted (A), axial T1-weighted (B), and T2weighted (C) images showing posterior epidural collection on the right side (arrow) at C5-6 level compressing the cord. This collection is hyperintense on T1-weighted and T2-weighted images and periphery is stained with hemosiderin (arrowhead)

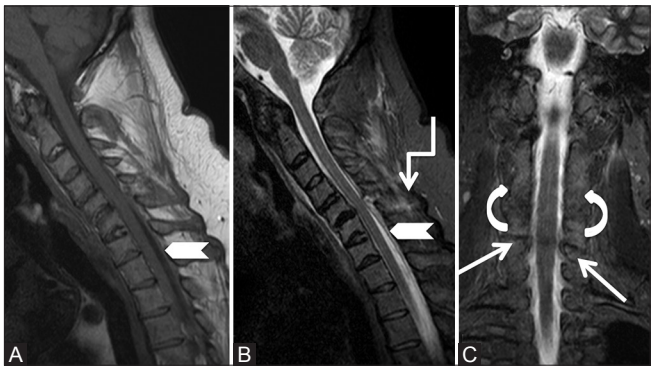

Figure 24a (A-C): Miscellaneous: Post-traumatic epidural hematoma: 43-year-old male with a known history of ankyosing spondylitis had a trivial fall followed with severe cervical region pain. Sagittal T1-weighted (A), T2-weighted (B) and short T1 inversion recovery (C) images showing loss of cervical lordosis, syndesmophytes along vertebral bodies, as well as osseous fusion of facets on both sides (curved arrow). Posterior epidural soft tissue is seen from C4-T1 levels (arrowhead) indenting on the cord and fracture is seen through C5-6 facet joint (arrow). Edema is seen in interspinous soft tissue (elbow arrow)

the heart when there is obstruction of IVC. Most important of these pathways is the deep pathway that recruits the ascending lumbar veins (which originates from common iliac veins) and anastomose with azygous vein on the right side and hemiazygyous vein on the left side.[57] The vertebral venous plexus of Batson, which includes the intervertebral veins and epidural venous plexus, also provides collateral pathway and communicates with the azygous system.[58] Enlarged and engorged epidural venous plexus can compress on the cord and nerve roots resulting in backache and radicular symptoms, as reported by Paksoy *et al*. in 13 patients with IVC obstruction [Figure 25].[7]

Extramedullary hemopoiesis

Chronic anemic states may be associated with extramedullary hematopoiesis which commonly involves liver, spleen, kidneys, and paraspinal location in posterior mediastinum.[59-62] Rarely, it may occur in the epidural space resulting in cord compression.

MRI is the imaging modality of choice for better delineation of the lesion due to better soft tissue resolution. Extramedullary hematopoiesis appears as well-defined lobulated masses embedded in the epidural space. These show isointense signal to cord on T1W, variable signal on T2W, and none-to-minimal post-contrast enhancement. Vertebrae may show diffuse marrow abnormality.[63]

Epidural hematopoiesis may occur due to the extrusion of blood forming elements from vertebral bodies into the epidural space through the weakened trabeculae or from the stimulation of embryonic rests in epidural space.[62]

Hirayama's disease

It is a flexion-induced myelopathy predominantly affecting C8–T1 in an asymmetric manner.[64] The ventral displacement of taut dura during flexion causes cord compression and microcirculatory changes.[64,65] The disease activity, however, attains a plateau after an initial insidiously progressive course.[66]

MRI is the imaging modality of choice to diagnose Hirayama's disease. Since the pathology is brought about by flexion of the cervical spine; presence of subtle signs on imaging in neutral position should prompt consideration of dynamic study.[64-66] Imaging features in a neutral position include loss of attachment of dura to lamina,[64] asymmetric lower cervical cord atrophy with increase in T2 signal, and loss of cervical lordosis.[64-66] Loss of dural attachment has been ranked with 100% specificity, and its presence in a young male with distal upper extremity weakness makes the diagnosis of Hirayama's disease likely.[64] However, the caveat is the presence of this sign in approximately half of normal healthy volunteers.[67] Further, this finding may be absent once the disease enters a stable phase.[65] Flexion MRI reveals forward migration of dura with enlargement of posterior epidural space seen as a crescentic region of high signal both on T1 and T2.[64-67] There may be congested

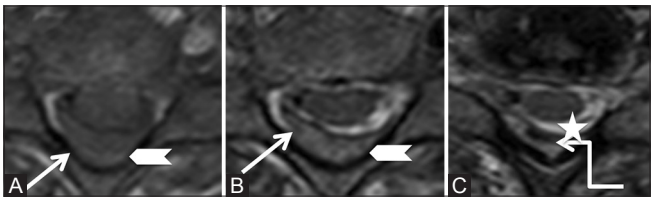

Figure 24b (A-C): Miscellaneous: Post-traumatic epidural hematoma: Axial T1-weighted (A), T2-weighted (B,C) images showing posterior epidural soft tissue (arrowhead) appearing hypointense on T1-weighted, hyperintense on T2-weighted, and showing hemosiderin foci within (star). It indents on the right hemicord

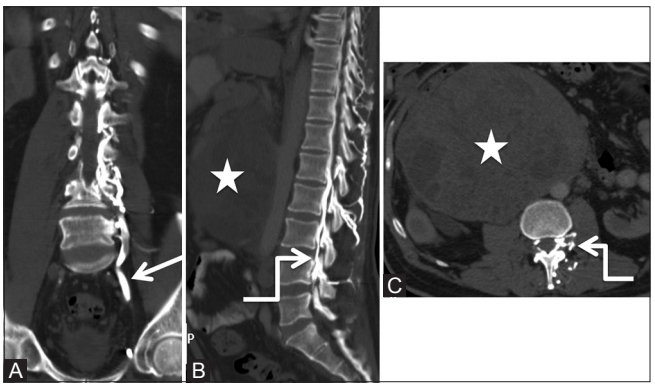

Figure 25 (A-C): Miscellaneous: Collateral venous pathway: Coronal (A), sagittal (B), and axial (C) Computed tomography scan images of the abdomen showing dilated ascending lumbar vein (arrow), anterior, and posterior epidural plexuses (elbow arrow) due to the chronic obstruction of inferior vena cava caused by metastatic retroperitoneal lymphadenopathy (star) from seminoma in a 50-year-old patient

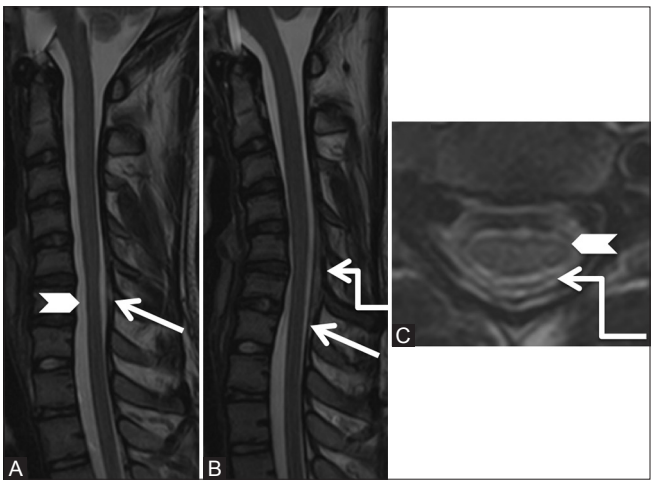

Figure 26 (A-C): Miscellaneous: Hirayama's disease: 15-year-old male had a history of progressive left upper limb weakness and wasting since 6 months. Sagittal T2-weighted images in neutral (A) position shows atrophy of the cervical cord from C5-7 levels (arrowhead) and subtle forward migration of the posterior dura (arrow), which is exaggerated in flexion (B) position. Axial T2-weighted (C) image at C5-6 level shows asymmetric atrophy of the left side of the cord (arrowhead), with widened posterior epidural space (elbow arrow)

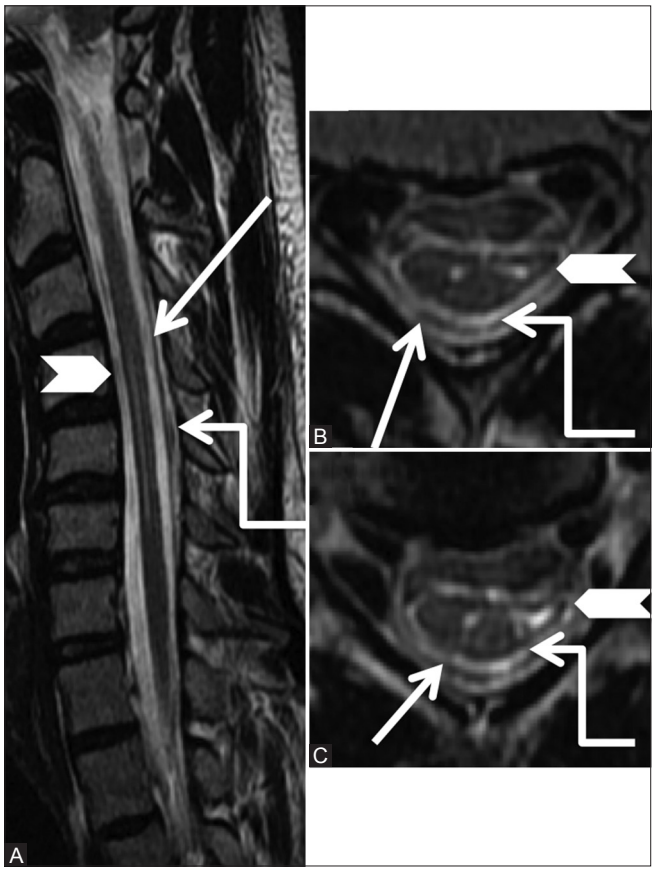

Figure 27 (A-C): Miscellaneous: Hirayama's disease: Sagittal T2-weighted (A) image in the flexion position shows atrophy of the cervical cord with hyperintense signal from C4-6 levels (arrowhead) and forward migration of the posterior dura (arrow). Axial T2-weighted (B, C) images at C5-6 level shows asymmetric atrophy of the left side of the cord with myelomalacic changes along with widened posterior epidural space (elbow arrow)

vessels in posterior epidural space (flow voids) better appreciated on constructive interference in steady state images.[66] Following contrast administration, the space shows uniform enhancement [Figures 26 and 27].

Hirayama's disease needs to be differentiated from amyotrophic lateral sclerosis and multifocal motor neuropathy of C8–T1.[64,65] In addition, disease progression may be prevented by application of a cervical collar during active phase of the disease.[66]

Conclusion

A clear understanding of the normal anatomy and early diagnosis of various pathological lesions in spinal posterior epidural space based on imaging findings is extremely important because these encroach on spinal cord or nerve root and may result in neurological sequelae.

Financial support and sponsorship
Nil.

Conflicts of interest
There are no conflicts of interest.

References

1. Chhabra A, Batra K, Satti S, Patel S, *et al*. Spinal epidural space: Anatomy, normal variations and pathological lesions on MR Imaging. Neurographics: Volume 2005, Issue 1:26:1-13.
2. Bromage PR. Anatomy. In: Bromage PR, editor. Epidural Analgesia. Philadelphia: WB Saunders; 1978. p. 8-20.
3. Hogan Q. Lumbar epidural anatomy: A new look by cryomicrotome section. Anesthesiology 1991:75:767-75.
4. Nickallis RW, Kokri MS. The width of posterior epidural space in obstetric patients. Anesthesia 1986;41:432-3.
5. Reina MA, Franco CD, Lopez A, De Andres JA, van Zundert A. Clinical implications of epidural fat in the spinal canal. A scanning electron microscopic study. Acta Anaesthesiol Belg 2009;60:7-17.
6. Batson, OV. Function of vertebral veins and their role in the spread of metastases. Ann Surg 1940;112:138-49.
7. Paksoy Y, Gormus N. Epidural venous plexus enlargements presenting with radiculopathy and back pain in patients with inferior vena cava obstruction or occlusion. Spine 2004;29:2419-24.
8. Richardson J, Groen GJ. Applied epidural anatomy. Continuing Educ Anaesth Crit Care Pain 2005;5:98-100.
9. Chen CY, Chuang YL, Yao MS, Chiu WT, Chen CL, Chan WP. Posterior epidural migration of a sequestrated lumbar disk fragment: MR imaging findings. AJNR Am J Neuroradiol 2006;27:1592-4.
10. Yahia LH, Newman N, Rivard CH. Light and scanning electron microscopy of human spinal ligamentum flavum. A preliminary study. Spine 1990;15:262-8.
11. Sairyo K, Biyani A, Goel VK, Leaman DW, Booth R Jr, Thomas J, *et al*. Ligamentum flavum hypertrophy due to accumulation of inflammation-related scar tissue. Spine 2007;32:E340-7.
12. Munns JJ, Lee JYB, Espinoza Orías AA, Takatori R, Andersson GB, An HS, *et al*. Ligamentum Flavum Hypertrophy in Asymptomatic and Chronic Low Back Pain Subjects. PLoS One 2015;10:e0128321.
13. Weishaupt D, Zanetti M, Boos N, Hodler J. MR imaging and CT in osteoarthritis of the lumbar facet joints. Skeletal Radiol 1999;28:215-9.
14. Taha H, Bareksei Y, Albanna W, Schirmer M. Ligamentum flavum cyst in the lumbar spine: A case report and review of the literature. J Orthop Traumatol 2010;11:117-22.
15. Bydon A, Su R, Parker S, McGirt MJ, Bydon M, Gojasian ZL, *et al*. Recurrent back and leg pain and cyst reformation after surgical resection of spinal synovial cysts: Systematic review of reported postoperative outcomes. Spine J 2010;10:820-6.
16. Liu SS, Williams KD, Drayer BP, Spetzler RF, Sonntag VK. Synovial cysts of the lumbosacral spine: Diagnosis by MR imaging. AJR Am J Roentgenol 1990;154:163-6.
17. Mahallati H, Wallace CJ, Hunter KM, Bilbao JM, Clark AW. MR imaging of a hemorrhagic and granulomatous cyst of the ligamentum flavum with pathologic correlation. AJNR Am J Neuroradiol 1999;20:1166-8.
18. Epstein NE, Baisden J. The diagnosis and management of synovial cysts: Efficacy of surgery versus cyst aspiration. Surg Neurol Int 2012;3(Suppl 3):S157-66.
19. Van Bergen J, Plazier M, Baets J, Simons PJ. An extensive spinal epidural abscess successfully treated conservatively. J Neurol Neurosurg Psychiatry 2009;80:351-3.
20. Chao D, Nanda A. Spinal epidural abscess: A diagnostic challenge. Am Fam Physician 2002;65:1341-6.

21. Darouiche RO, Hamill RJ, Greenberg SB, Weathers SW, Musher DM. Bacterial spinal epidural abscess. Review of 43 cases and literature survey. Medicine 1992;71:369-85.
22. Mackenzie AR, Laing RB, Smith CC, Kaar GF, Smith FW. Spinal epidural abscess: The importance of early diagnosis and treatment. J Neurol Neurosurg Psychiatry 1998;65:209-12.
23. Martin RJ, Yuan HA. Neurosurgical care of spinal epidural, subdural, and intramedullary abscesses and arachnoiditis. Orthop Clin North Am 1996;27:125-36.
24. Reihsaus E, Waldbaur H, Seeling W. Spinal epidural abscess: A meta-analysis of 915 patients. Neurosurg Rev 2000;23:175-204.
25. Auletta JJ, John CC. Spinal epidural abscesses in children: A 15-year experience and review of the literature. Clin Infect Dis 2001;32:9-16.
26. Chauhan A, Gupta BB. Spinal tuberculosis. Indian Acad Clin Med 2007;8:110-4.
27. Moorthy S, Prabhu NK. Spectrum of MR imaging findings in spinal tuberculosis. AJR Am J Roentgenol 2002;179:979-83.
28. Ansari S, Amanullah MF, Ahmad K, Rauniyar RK. Pott's spine: Diagnostic imaging modalities and technology advancements. N Am J Med Sci 2013;5:404-11.
29. Arora S, Sabat D, Maini L, Sural S, Kumar V, Gautam VK, *et al*. Isolated involvement of the posterior elements in spinal tuberculosis: A review of twenty-four cases. J Bone Joint Surg Am 2012;94:e151.
30. Quint DJ, Boulos RS, Sanders WP, Mehta BA, Patel SC, Tiel RL. Epidural lipomatosis. Radiology 1988;169:485-90.
31. Fogel GR, Cunningham PY 3rd, Esses SI. Spinal epidural lipomatosis: Case reports, literature review and meta-analysis. Spine J 2005;5:202-11.
32. Geers C, Lecouvet FE, Behets C, Malghem J, Cosnard G, Lengelé BG. Polygonal deformation of the dural sac in lumbar epidural lipomatosis: Anatomic explanation by the presence of meningovertebral ligaments. AJNR Am J Neuroradiol 2003;24:1276-82.
33. Rajput D, Srivastava AK, Kumar R. Spinal epidural lipomatosis: An unusual cause of relapsing and remitting paraparesis. J Pediatr Neurosci 2010;5:150-2.
34. Badve CA, Khanna PC, Phillips GS, Thapa MM, Ishak GE. MRI of closed spinal dysraphisms. Pediatr Radiol 2011;41:1308-20.
35. Leu NH, Chen CY, Shy CG, Lu CY, Wu CS, Chen DC, *et al*. MR imaging of an infiltrating spinal epidural angiolipoma. AJNR Am J Neuroradiol 2003;24:1008-11.
36. Kuroda S, Abe H, Akino M, Iwasaki Y, Nagashima K. Infiltrating spinal angiolipoma causing myelopathy: Case report. Neurosurgery 1990;27:315-8.
37. Hu S, Hu CH, Hu XY, Wang XM, Dai H, Fang XM, *et al*. MRI Features of Spinal Epidural Angiolipomas. Korean J Radiol 2013;14:810-7.
38. Zhong W, Huang S, Chen H, Sun H, Cai B, Liu Y, *et al*. Pure spinal epidural cavernous hemangioma. Acta Neurochir 2012;154:739-45.
39. Lee JW, Cho EY, Hong SH, Chung HW, Kim JH, Chang KH, *et al*. Spinal epidural hemangiomas: Various types of MR imaging features with histopathologic correlation. AJNR Am J Neuroradiol 2007;28:1242-8.
40. Goyal M, Willinsky R, Montanera W, terBrugge K. Paravertebral arteriovenous malformations with epidural drainage: Clinical spectrum, imaging features, and results of treatment. AJNR Am J Neuroradiol 1999;20:749-55.
41. Chen CJ, Huang CC, Hsu YY, Hsu WC. Small isolated paraspinal arteriovenous fistula. AJNR Am J Neuroradiol 1997;18:359-61.
42. Cognard C, Semaan H, Bakchine S, Miaux Y, Thibault S, Sola Martinez MT, *et al*. Paraspinal arteriovenous fistula with perimedullary venous drainage. AJNR Am J Neuroradiol 1995;16:2044-8.
43. Liu JK, Cole CD, Kan P, Schmidt MH. Spinal extradural arachnoid cysts: Clinical, radiological, and surgical features. Neurosurg Focus 2007;22:1-5.
44. Choi SW, Seong HY, Roh SW. Spinal extradural arachnoid cyst. J Korean Neurosurg Soc 2013;54:355-8.
45. Nabors MW, Pait TG, Byrd EB, Karim NO, Davis DO, Kobrine AI, *et al*. Updated assessment and current classification of spinal meningeal cysts. J Neurosurg 1988;68:366-77.
46. Payer M, Brühlhart K. Spinal extradural arachnoid cyst: Review of surgical techniques. J Clin Neurosci 2011;18:559-60.
47. Silva JR Jr1, Hayashi D, Yonenaga T, Fukuda K, Genant HK, Lin C, *et al*. MRI of bone marrow abnormalities in hematological malignancies. Diagn Interv Radiol 2013;19:393-9.
48. Li MH, Holtås S, Larsson EM. MR imaging of spinal lymphoma. Acta Radiol 1992;33:338-42.
49. Cugati G, Singh M, Pande A, Ramamurthi R, Balasubramanyam M, Sethi SK, *et al*. Primary spinal epidural lymphomas. J Craniovertebr Junction Spine 2011;2:3-11.
50. Klimo *P* Jr, Schmidt MH. Surgical management of spinal metastases. Oncologist 2004;9:188-96.
51. Shah LM, Salzman KL. Imaging of Spinal Metastatic Disease. Int J Surg Oncol 2011;2011:769753.
52. Fukui MB, Swarnkar AS, Williams RL. Acute spontaneous spinal epidural hematomas. AJNR Am J Neuroradiol 1999;20:1365-72.
53. Baek BS, Hur JW, Kwon KY, Lee HK. Spontaneous spinal epidural hematoma. J Korean Neurosurg Soc 2008;44:40-2.
54. Foo D, Rossier AB. Post-traumatic spinal epidural hematoma. Neurosurgery 1982;11 (1 Pt 1):25-32.
55. Domenicucci M, Ramieri A, Ciappetta P, Delfini R. Nontraumatic acute spinal subdural hematoma: Report of five cases and review of the literature. J Neurosurg 1999;91:65-73.
56. Chen C, Ro L. Central gadolinium enhancement of an acute spontaneous spinal epidural hematoma. Neuroradiology 1996;38:114-6.
57. Sonin AH, Mazer MJ, Powers TA. Obstruction of the inferior vena cava: A multiple-modality demonstration of causes, manifestations, and collateral pathways. Radiographics 1992;12:309-22.
58. Umeoka S1, Koyama T, Togashi K, Kobayashi H, Akuta K. Vascular dilatation in the pelvis: Identification with CT and MR imaging. Radiographics 2004;24:193-208.
59. Warshauer DM, Schiebler ML. Intrahepatic extramedullary hema- topoiesis: MR, CT, and sonographic appearance. J Comput Assist Tomogr 1991;15:683-5.
60. Fernbach SK, Feinstein KA. Extramedullary hematopoiesis in the kidneys in infant siblings with myelofibrosis. Pediatr Radiol 1992;22:211-2.
61. Moran CA, Suster S, Fishback N, Koss MN. Extramedullary hematopoiesis presenting as posterior mediastinal mass: A study of four cases. Mod Pathol 1995;8:249-51.
62. Dibbern DA Jr, Loevner LA, Lieberman AP, Salhany KE, Freese A, Marcotte PJ. MR of thoracic cord compression caused by epidural extramedullary hematopoiesis in myelodysplastic syndrome. AJNR Am J Neuroradiol 1997;18:363-6.
63. Garg K, Singh PK, Singh M, Chandra PS, Sharma BS. Long segment spinal epidural extramedullary hematopoiesis. Surg Neurol Int 2013;4:161.
64. Lehman VT, Luetmer PH, Sorenson EJ, Carter RE, Gupta V, Fletcher GP, *et al*. Cervical spine MR imaging findings of patients with Hirayama disease in North America: A multisite study. AJNR Am J Neuroradiol 2013;34:451-6.
65. Gandhi D, Goyal M, Bourque PR, Jain R. Case 68: Hirayama disease. Radiology 2004;230:692-6.
66. Raval M, Kumari R, Dung AA, Guglani B, Gupta N, Gupta R. MRI findings in Hirayama disease. Indian J Radiol Imaging 2010;20:245-9.
67. Vargas MC, Castillo M. Magnetic resonance imaging in Hirayama disease. J Radiol Case Rep 2011;5:17-23.